

Changing the prior: absolute neutrino mass constraints in nonlocal gravity*

Yves Dirian^{1,†}

¹*Département de Physique Théorique and Center for Astroparticle Physics,
Université de Genève, 24 quai Ansermet, CH-1211 Genève 4, Switzerland*

Prior change is discussed in observational constraints studies of nonlocally modified gravity. In the latter, a model characterized by a modification of the form $\sim m^2 R \square^{-2} R$ to the Einstein-Hilbert action was compared against the base Λ CDM one in a Bayesian way. It was found that the competing modified gravity model is significantly disfavored (at 22 : 1 in terms of betting-odds) against Λ CDM given CMB+SN Ia+BAO data, because of a dominant tension appearing in the $H_0 - \Omega_M$ plan. We identify the underlying mechanism generating such a tension and show that it is mostly caused by the late-time, quite smooth, phantom nature of the effective dark energy described by the nonlocal model. We find possible solutions for it to be resolved and explore a given one that consists in extending the initial baseline from one massive neutrino eigenstate to three degenerate ones, whose absolute mass $\sum m_\nu/3$ is allowed to take values within a reasonable prior interval. As a net effect, the absolute neutrino mass is inferred to be non-vanishing at 2σ level, best-fitting at $\sum m_\nu \approx 0.21$ eV, and the Bayesian tension disappears rendering the nonlocal gravity model statistically equivalent to Λ CDM, given recent CMB+SN Ia+BAO data. We also discuss constraints from growth rate measurements $f\sigma_8$ whose fit is found to be improved by a larger massive neutrino fraction as well. The ν -extended nonlocal model also prefers a higher value of H_0 than Λ CDM, therefore in better agreement with local measurements. Our study provides one more example suggesting that the neutrino density fraction Ω_ν is partially degenerated with the nature of the dark energy. This emphasizes the importance of cosmological and terrestrial neutrino research and, as a massive neutrino background impacts structure formation observables non-negligibly, proves to be especially relevant for future galaxy redshift surveys.

I. INTRODUCTION

Modern cosmology has undergone fast developments over the past two decades. These advances were originally built on theoretical insights originating from Einstein's theory of General Relativity (GR) that has now been extensively tested on solar system and terrestrial scales [1]. Until now, no significant deviations from GR have been observed into such regimes. On cosmological, far-infrared ones, the theory provides the bedrock of the standard cosmological model whose construction has mostly been driven by increasingly precise cosmological data collection, legitimating it as a precision science. In particular, observation of distant Type Ia supernovae [2, 3] led to the abandon of the inflationary cold dark matter (CDM) paradigm (see e.g. [4]) and to the birth of the Λ CDM one – consisting in allowing the cosmological constant Λ to take non-trivial values in CDM. Such a model extension adds an overwhelming, thereby constant, dark energy component to the corresponding homogeneous and isotropic Friedmann-Lemaître-Robertson-Walker (FLRW) universe and at the same time raises fundamental theoretical questions about its origin, late-time domination and naturalness [5, 6]. The idea of modelling differently such a component for addressing these issues keeps to be actively explored nowadays through different perspectives (see e.g. [7–10] for recent reviews). Among these, there are strategies aiming to modified the gravitational Einstein-Hilbert action itself, evading Lovelock's theorem [11, 12]. For instance, one finds higher-derivative

gravity [13], the five-dimensional Dvali-Gabadadze-Porrati (DGP) braneworld model [14], scalar-vector-tensor gravity [15], massive gravity [16, 17], bi- [18] and multi- [19] gravity (see [20] for a review), scalar-tensor Effective Field Theories of dark energy [21, 22], which all have a common thread in that they are local. Nevertheless, nonlocal modifications of GR have also attracted much interest over the years. At the classical level, these are formally characterized by the fact that the value of the Lagrange density $\mathcal{L}[\phi_i]$ (or equivalently of the corresponding equations of motion) at a given point in space-time depends on the whole history to which the fields ϕ_i have been subject to within the past lightcone of that point. Typically, these are manifested by the presence of non-analytic operators into the action which generically provide good candidates for modifying the theory in its infrared regime. These are motivated by radiative corrections induced by gravity or light-matter components on curved spacetime [23–25], also responsible for the trace anomaly [26, 27] or non-perturbative effects giving raise to a scale dependent Newton's constant [28–32], but also by renormalizability and singularity issues in higher-derivative theories of gravity [33, 34] or string inspired scenarios [35, 36]. Models have also been proposed in a bottom-up approach for appreciating the effects of various types of nonlocal operators within the cosmological context [37–50]. Ultimately, if its phenomenology appears to be satisfying, a parametric model will be presented for competing against the Λ CDM one in a Bayesian statistical perspective [51, 52], given the data at hand.

Two nonlocal models of this sort have been recently proposed, one of which is characterized by the addition of a term $\sim m^2 (g_{\mu\nu} \square^{-1} R)^T$ to Einstein's equations [43], whereas a second one modifies the Einstein-Hilbert action by a term $\sim m^2 R \square^{-2} R$ [45]. Their effective dark energy phenomenology has been studied in Ref. [53] where it was found that

* Based on observations obtained with Planck (<http://www.esa.int/Planck>), an ESA science mission with instruments and contributions directly funded by ESA Member States, NASA, and Canada.

† Electronic address: yves.dirian@unige.ch

both models describe a quite smooth, phantom dark energy component emerging at late-times, possessing an equation-of-state today of $w_{\text{DE}} = -1.04$ and $w_{\text{DE}} = -1.15$ respectively, and a fifth force that enhances the clustering of linear structures compared to that in ΛCDM : at $\lesssim 6\%$ level in the linear matter power spectrum around the BAO scale (see also Ref. [54] where nonlinear structure formation through N-body simulation has been studied for the model of Ref. [45]). Observational constraints using Bayesian techniques were then carried out in Refs. [55, 56] in a complementary perspective [57, 58], i.e. using cosmological data from Cosmic Microwave Background (CMB), Baryon Acoustic Oscillations (BAO) and Type Ia supernova (SNIa) observations. Constraints on the linear growth rate of structures were also obtained a posteriori, that is, constraining the quantity $f\sigma_8$ derived from both nonlocal models with Redshift-Space Distortions (RSD) measurements once the linear matter power spectrum has been calibrated on the bestfit inferred from CMB+SNIa+BAO data. The joined CMB+SNIa+BAO constraints showed that, provided a prior parametrization fixed on the so-called *Planck* 2015 baseline [59], the model of Ref. [43] is indistinguishable from standard ΛCDM with a Bayes factor of 1.0, whereas the one presented in Ref. [45] is significantly disfavored with a Bayes factor of 22.7. The latter discrepancy was shown to result from a severe CMB-SNIa tension appearing in the $H_0 - \Omega_M$ plane, breaking the nonlocal models' concordance given the data.

In this article, we analyze in more details the origin of this tension and find solutions for resolving it. In particular, we will see that changing the neutrino sector of the aforementioned baseline from one dominant active mass-eigenstate to three degenerated ones, in conjunction with a larger prior put on the corresponding absolute neutrino mass, restores the concordance of the nonlocal model to a non-negligible extent. Effectively, such a resolution exploits degeneracies between modified gravity effects of the nonlocal model and those caused by a more massive neutrino component. Similar degeneracies have already been noticed in local modified gravity theories, for instance at linear level in TeVeS [60], covariant galileons [61], K -mouflage [62] and recently in Horndeski models [63], but also at the nonlinear one through N-body simulations of $f(R)$ scenarios in Ref. [64].

The rest of this paper is organized as follows. The specific nonlocal gravity model we consider will briefly be reviewed in section II. In section III, we expose how the latter is embedded into a statistical model, given specific data that we also present. Furthermore, we specify our prior parametrization and justify such a choice from empirical evidences. Section IV presents the results drawn from observational constraints, attempts for a comprehensive analysis of the resolution of the aforementioned tension and quantifies it using Bayesian model comparison methods. We present a summary of our work in section V before we conclude.

II. THE RR NONLOCAL GRAVITY MODEL

In this section, we briefly introduce the nonlocal gravity model originally proposed by Ref. [45] which, following Ref. [56] for convenience, will be referred to as the RR model. Our conventions, notations and strategy to solve the equations are similar to that of Refs. [53, 56], that the interested reader is invited to consult for more details.

The RR model is defined through an extension of the Einstein-Hilbert action reading,

$$S_{RR} = \frac{1}{16\pi G} \int d^4x \sqrt{-g} \left[R - \frac{m^2}{6} R \square^{-2} R - \mathcal{L}_m \right], \quad (1)$$

where \mathcal{L}_m is the Lagrange density of minimally coupled matter fields and the \square^{-1} operator is a formal notation for a Green's function of the curved-space d'Alembert one $\square \equiv \nabla^\mu \nabla_\mu$. Since the kernel of \square is non-trivial such a Green's function is not unique and its precise structure while appearing in Eq. (1) is not known, as well as the origin of the mass scale m . This originates from the fact that this model was built through a bottom-up approach and its embedding into a more fundamental framework still remains under investigation [65, 66], see also Ref. [67] for a recent review. From a more technical point of view, several subtleties arise from the presence of \square^{-1} into an action. One of them concerns the causal character of the classical evolution governed by the corresponding Euler-Lagrange equations and has been discussed in details in the literature (see e.g. Refs. [29, 68]). Another one ties to the “localized” version of the action (1), most conveniently used for computing the corresponding cosmology without having to deal with less manipulable integro-differential systems. The results exposed below are obtained from such a local version taken to be ¹,

$$S_{RR,\text{loc}} = \frac{1}{16\pi G} \int d^4x \sqrt{-g} \left[R - \frac{m^2}{6} R V - \xi_1 (\square U + R) - \xi_2 (\square V + U) - \mathcal{L}_m \right], \quad (2)$$

where U and V are two “auxiliary” scalar fields and $\xi_{1,2}$ are Lagrange multipliers enforcing the constraints,

$$\square U = -R, \quad (3)$$

$$\square V = -U. \quad (4)$$

sourcing the latter. Invoking a given (left) inverse, one can solve the latter formally in simply writing,

$$U = -\square^{-1} R, \quad (5)$$

$$V = -\square^{-1} U = \square^{-2} R, \quad (6)$$

which allows one to integrate U , V out from the action (and $\xi_{1,2}$ in a similar way), leading back to the nonlocal action (1).

¹ See also Ref. [69] where another localization has been proposed.

The same procedure can be applied at the level of the equations of motion that are,

$$G_{\mu\nu} - \frac{m^2}{6} K_{\mu\nu} = 8\pi G T_{\mu\nu}, \quad (7)$$

$$\square U = -R, \quad (8)$$

$$\square V = -U, \quad (9)$$

with

$$K_{\mu\nu} \equiv 2VG_{\mu\nu} - 2\nabla_\mu \nabla_\nu V - 2\nabla_{(\mu} U \nabla_{\nu)} V + \left(2\square V + \nabla_\alpha U \nabla^\alpha V - \frac{U^2}{2} \right) g_{\mu\nu}, \quad (10)$$

where $T^{\mu\nu} \equiv (2/\sqrt{-g}) \delta(\mathcal{L}_m \sqrt{-g}) / \delta g_{\mu\nu}$ is the matter source. In writing Eqs. (5) and (6) at that stage, causality of the classical dynamics requires that the source-convolving kernels used are all of the retarded kind and, in accordance with their artificial nature, that the auxiliary fields possess no homogeneous (i.e. free) solutions [42, 43, 45, 69–74], at least into the *in* state. This uniquely fixes the inverse of \square used in integrating out U and V and catches the classical solutions that we are interested in in that work. At the “localized” level, trivial homogeneous modes for the auxiliary fields is realized in fixing vanishing values for U and V and their time derivatives on the initial hypersurface. Here we interpret these requirements as theory-level data that one should supplement to the local action (2) from the beginning, and changing these prescriptions changes the underlying nonlocal model.

According to the procedure used until now [53, 56, 75], we set the initial hypersurface deep into the radiation dominated era (RD). During this period at the background level, the curvature scalar is sub-dominating compared to the overall energy scale of the process so one can naively set the space-averaged value $\bar{R}|_{\text{RD}} \simeq 0$ and see that the resulting $\bar{U}, \bar{V}|_{\text{RD}}$ are therefore not sourced, and remain small. Linear perturbations $\delta U, \delta V|_{\text{RD}}$ induced by gravitational ones remain also so [69]. However once matter starts to dominate over radiation, the latter quantities acquire a non-trivial dynamics leading to the emergence of a late time, quite smooth dynamical dark energy component [53] driving the accelerated expansion of the Universe which ends up into a Big Rip [69, 76]. For being ultimately legitimate, this choice of initial conditions needs to assume that the secular growth of U and V during earlier stages of the Universe is mild enough for not strongly affecting the vanishing values chosen while starting in RD. For the case of inflationary scenarios, it can be argued that the additional term in Eq. (1) is suppressed by the corresponding inflationary energy scale, since it only modifies the theory into the far-infrared. In any case this question deserves a special attention and a more quantitative analysis is needed (see Refs. [48, 65, 77] where such a scenario was considered). Of course, the configuration reached by the auxiliary fields in RD will depend on the particular model of inflation assumed but also on other processes affecting the scalar curvature within the primordial Universe such as the electroweak or QCD phase transition, conformal anomalies, or during RD itself through the presence of thermalized Standard Model massive particles [78]. This issue was recently anticipated in Ref. [79] where

the authors studied the effect of varying the auxiliary fields’ initial conditions deep into RD over a broad range of values, unveiling in particular the existence of another phenomenologically viable cosmology of the nonlocal model (1).

We close this description in emphasizing that, from a statistical perspective which will be taken in the following, fixing vanishing initial conditions for the auxiliary fields is a *modelling assumption* or *theoretical prior* (much as pretending that Λ -dark energy is replaced by the RR one in our context). Therefore, the only remaining free parameter added to the Einstein-Hilbert action is the mass scale m , whose value is to be fixed from Universe’s spatial flatness condition – similarly of fixing of the value of Λ in flat Λ CDM models. The model has therefore the same number of free parameters as Λ CDM.

III. COSMOLOGICAL MODELS

The cosmological models incorporating Λ - and RR -dark energies considered in this article are one-parameter extensions of those studied in Ref. [56] and are similarly tested within a Bayesian framework.

In this section, we therefore only provide a brief, self-contained review of the datasets and parametrization used and refer the reader to the above reference, and references therein, for further details about their structure and construction. Technical details relative to the equations and numerical implementation used can be found in Sec. 2 and App. A. of the latter reference.

A. Datasets

For performing our global fit we utilize distant Type Ia supernovae (SNIa) observations complemented with Cosmic Microwave Background (CMB) data and distance measurements from several Baryon Acoustic Oscillations (BAO) surveys. Together with CMB lensing data, SNIa and BAO observations allow to apply constraints on the late time expansion of the Universe in breaking further primary CMB degeneracies. We will then discuss a posteriori constraints on the growth rate from Redshift-Space Distortions (RSD) measurements.

The CMB dataset we consider comes from the *Planck* satellite mission and is made of the *lowTEB* power spectra data for multipoles $\ell \leq 29$, the high- ℓ TT, TE and EE ones for $\ell > 29$ [80], as well as the data relative to the power spectrum of the reconstructed CMB lensing potential [81], in the following the latter will be referred to as the *Planck* dataset. For the BAO data, we include the isotropic measurements reported in Ref. [82] at $z_{\text{eff}} = 0.106$ from 6dFGS and Ref. [83] at $z_{\text{eff}} = 0.15$ from SDSS-MGS DR7, as well as the anisotropic ones of Ref. [84] from the LOWZ ($z_{\text{eff}} = 0.32$) and CMASS ($z_{\text{eff}} = 0.57$) samples from BOSS. The SNIa data we use are those of the SDSS-II/SNLS combined analysis (also known as *JLA*), which comprises 740 objects at $z \lesssim 1$ [85].

Below we study constraints with two dataset combinations: (i) *Planck* and (ii) the combined CMB, BAO and SNIa data, which we shall refer to as the *BAPJ* dataset to preserve the nomenclature of Ref. [56].

B. Parametrization and prior specification

In accordance with the use of the above measurements, the complement of the dark energy sector of the models considered in this paper are defined following the so-called *Planck* 2015 *baseline* [59]. Regarding the radiation/matter content of the Universe, ionization history and primordial initial conditions, the baseline assumes a particular modelling that has now become the standard cosmological setting on which is built the *base* Λ CDM model. Predictions from such a model are computed in using a cosmological linear Einstein-Boltzmann code such as CAMB [86] or CLASS [87]. In our study, we make use of the latter and provide a modified version of it on GITHUB (see [88] for the link) which includes the *RR* gravity model introduced in the previous subsection. Bayesian parameter extraction and model selection are carried out with the Markov Chain Monte Carlo (MCMC) code MONTEPYTHON [89] originally interfaced with CLASS.

The baseline specifies a continuous 6-dimensional parametrization which can be provided by the vector,

$$\theta_{\text{base}} = (H_0, 100\omega_b, \omega_{\text{cdm}}, \ln(10^{10}A_s), n_s, \tau), \quad (11)$$

with $H_0 \equiv 100h$ km/s/Mpc the Hubble expansion rate today, $\omega_i \equiv \Omega_i h^2$ where Ω_i is the present energy density fraction of baryons ($i = b$) and cold dark matter ($i = \text{cdm}$), A_s and n_s are the amplitude and spectral tilt of the primordial fluctuations and τ the optical depth to reionization. Below will also appear derived quantities being Ω_m the total matter density fraction today, σ_8 the root mean square linear fluctuation in the mass distribution in objects of radius 8 Mpc/h at $z = 0$ and the dark energy densities Ω_Λ , Ω_{RR} corresponding to the Λ CDM and *RR* models respectively. The latter are determined in requiring a vanishing spatial curvature of the Universe $\Omega_K = 0$ and this is done in adequately tuning the parameter controlling the dark energy density within the model specified: Λ in Λ CDM or m in *RR*. In this work we use improper flat prior with edges everywhere unbounded expect for the lower bound of the optical depth τ taken to be 0.01, in accordance with Gunn-Peterson trough observations (see e.g. Ref. [90]).

In the neutrino sector, the baseline assumes one dominant active neutrino species of fixed mass M_ν with prior,

$$P(M_\nu|\Lambda\text{CDM}) = \delta(M_\nu/\text{eV} - 0.06). \quad (12)$$

In CLASS, its temperature is accordingly tuned for reproducing predictions from neutrino decoupling computations [91]. The latter species is supplemented with a massless neutrino one whose effective number of degrees-of-freedom is adjusted so as to reproduce a total effective number of relativistic components of $N_{\text{eff}} = 3.046$ in the early Universe (see Refs. [92, 93] for recent reviews).

As will be justified more clearly below, the extension we consider in this work assumes three active massive species respecting the same conditions. Moreover their corresponding mass-eigenstates are assumed to be degenerate, i.e. the sum of their masses respects $\sum m_\nu \equiv 3m_\nu$ so that we are only interested in the absolute neutrino mass, as this is allowed by the lack of sensitivity of the measurements considered in this work. We therefore adopt the following parametrization,

$$\theta_\nu = (H_0, 100\omega_b, \omega_{\text{cdm}}, \ln(10^{10}A_s), n_s, \tau, \sum m_\nu), \quad (13)$$

and the prior interval on the additional parameter is taken to be uniform and compact $\sum m_\nu \in [0, 5]$ eV, consistent with existing data (see subsection IV F for more details and references on the latter choice).

The cosmological models denoted by Λ CDM and *RR* are parametrized by θ_{base} while their extended versions build out of θ_ν will be called $\nu\Lambda$ CDM and νRR respectively.

IV. OBSERVATIONAL CONSTRAINTS AND MODEL COMPARISON

In this section, we present and study our observational constraints and model comparison results.

We start by analyzing some structural features of the *RR* model and, in comparing them to the ones of standard Λ CDM, explain the origin of the tensions first found in Ref. [75], given the nonlocal model. Then, we present the parameter constraints on the νRR model introduced above and discuss Bayesian model selection through the computation of various Bayes factors comparing pairs of the four above-mentioned models. We finally also discuss the merits of growth rate measurements for been able to constrain further the cosmologies at hand.

A. The origin of the CMB-SNIa tension given *RR*

1. *Planck* dataset

Table I summarizes the constraints on the Λ CDM and *RR* models obtained with the *Planck* dataset (first and third columns). The parameter shifts between the two models can be understood in comparing the relevant features in both models with each other.

A first noteworthy point is that the differences between results from parameter inference on both cosmologies are statistically non-significant ($\lesssim 1\sigma$) for all parameters in θ_{base} , with the exception of the background-related H_0 which undergoes the most significant shift ($\sim 5\sigma$). Notice that σ_8 , derived at the linear level, also undergoes a significant change ($\sim 3\sigma$). As already noticed in [54], the latter results from the enhanced clustering in the nonlocal model, mostly induced by a lower expansion rate (see top panel of Fig. 1) that reduces the Hubble friction to matter perturbations supplemented by, although to a milder level, a higher late-time gravitational strength modelled by a time-dependent effective Newton constant $G_{\text{eff}}(z, k)$, exhibiting scale-dependence in

TABLE I. Summary of the means, standard deviations and (effective) χ^2 goodness-of-fit values for the one-dimensional marginalized likelihood distributions of the Λ CDM, $\nu\Lambda$ CDM, RR and νRR models obtained with the *Planck* (left) and *BAPJ* (right) datasets. The $\Delta\chi^2$ values are taken with respect to the Λ CDM χ^2 values for each dataset, where $\chi^2 \equiv -2 \ln \mathcal{L}$, with \mathcal{L} being the likelihood function. All bounds shown correspond to 1σ .

	<i>Planck</i> Λ CDM	<i>Planck</i> $\nu\Lambda$ CDM	<i>Planck</i> RR	<i>Planck</i> νRR	<i>BAPJ</i> Λ CDM	<i>BAPJ</i> $\nu\Lambda$ CDM	<i>BAPJ</i> RR	<i>BAPJ</i> νRR
$100\omega_b$	$2.225^{+0.016}_{-0.016}$	$2.220^{+0.017}_{-0.017}$	$2.227^{+0.016}_{-0.016}$	$2.222^{+0.017}_{-0.017}$	$2.228^{+0.014}_{-0.015}$	$2.229^{+0.014}_{-0.015}$	$2.213^{+0.014}_{-0.015}$	$2.221^{+0.014}_{-0.015}$
ω_{cdm}	$0.1194^{+0.0014}_{-0.0015}$	$0.1198^{+0.0015}_{-0.0016}$	$0.1191^{+0.0015}_{-0.0015}$	$0.1196^{+0.0015}_{-0.0016}$	$0.1190^{+0.0011}_{-0.0011}$	$0.1189^{+0.0011}_{-0.0011}$	$0.1210^{+0.0010}_{-0.0010}$	$0.1197^{+0.0012}_{-0.0012}$
H_0	$67.50^{+0.65}_{-0.66}$	$66.12^{+2.1}_{-1.2}$	$71.51^{+0.81}_{-0.84}$	$69.57^{+2.5}_{-1.6}$	$67.67^{+0.47}_{-0.50}$	$67.60^{+0.66}_{-0.55}$	$70.44^{+0.56}_{-0.56}$	$69.49^{+0.79}_{-0.80}$
$\ln(10^{10} A_s)$	$3.064^{+0.025}_{-0.025}$	$3.080^{+0.030}_{-0.034}$	$3.047^{+0.026}_{-0.025}$	$3.071^{+0.032}_{-0.035}$	$3.066^{+0.019}_{-0.026}$	$3.071^{+0.026}_{-0.029}$	$3.027^{+0.027}_{-0.023}$	$3.071^{+0.032}_{-0.032}$
n_s	$0.9647^{+0.0048}_{-0.0049}$	$0.9637^{+0.0050}_{-0.0050}$	$0.9649^{+0.0049}_{-0.0049}$	$0.9639^{+0.0051}_{-0.0052}$	$0.9656^{+0.0041}_{-0.0043}$	$0.9661^{+0.0043}_{-0.0043}$	$0.9601^{+0.0040}_{-0.0039}$	$0.9635^{+0.0045}_{-0.0045}$
τ	$0.06530^{+0.014}_{-0.014}$	$0.07312^{+0.016}_{-0.018}$	$0.05733^{+0.014}_{-0.014}$	$0.06905^{+0.017}_{-0.018}$	$0.06678^{+0.011}_{-0.013}$	$0.06965^{+0.014}_{-0.015}$	$0.04516^{+0.014}_{-0.012}$	$0.06880^{+0.017}_{-0.017}$
$\sum m_\nu$ [eV]	0.06 (fixed)	< 0.249	0.06 (fixed)	< 0.278	0.06 (fixed)	< 0.10	0.06 (fixed)	$0.219^{+0.083}_{-0.084}$
σ_8	$0.8171^{+0.0089}_{-0.0089}$	$0.7949^{+0.033}_{-0.016}$	$0.8487^{+0.0097}_{-0.0096}$	$0.8212^{+0.038}_{-0.020}$	$0.8170^{+0.0076}_{-0.0095}$	$0.8157^{+0.013}_{-0.011}$	$0.8443^{+0.010}_{-0.0099}$	$0.8215^{+0.017}_{-0.017}$
$\Delta\chi^2_{Planck}$	0 ($\chi^2 = 12943.30$)	-0.04	-1.6	-1.6	0 ($\chi^2 = 12943.42$)	-0.14	-0.14	-1.52
$\Delta\chi^2_{BAO}$					0 ($\chi^2 = 4.42$)	0	2.48	2.38
$\Delta\chi^2_{JLA}$					0 ($\chi^2 = 683.2$)	-0.12	3.56	2.5
$\Delta\chi^2_{total}$	0 ($\chi^2 = 12943.30$)	-0.04	-1.6	-1.6	0 ($\chi^2 = 13631.04$)	-0.26	5.9	3.36

the far-infrared [56]. More clustering also increases the lensing power (see bottom panel of Fig. 1) and in turn smooths out temperature fluctuations more efficiently. Moreover, this requires a smaller primordial amplitude A_s which comes together with a delayed reionization epoch given that the CMB damping tail constrains well the combination $A_s e^{-2\tau}$ at high- ℓ . The nonlocal model also features a lower late-time integrated Sachs-Wolfe (ISW) effect compared to the one in Λ CDM (as displayed in Fig. 4 of [56]) favorable for it, but both clustering enhancements are responsible for an excess in the growth rate, penalizing the modified gravity model with respect to the standard one.

As already mentioned above and more importantly for our present purpose, the *Planck* dataset constraints H_0 to be larger in RR ($H_0 \approx 71.51 \pm 0.84$ km/s/Mpc) than in Λ CDM ($H_0 \approx 67.50 \pm 0.66$ km/s/Mpc). This preference for higher H_0 a fortiori originates from the late-time emerging, quite smooth and phantom nature of the RR effective dark energy compared to that modelled by a cosmological constant Λ . In the following we attempt to provide a comprehensive explanation of this fact. The Friedmann equation including a dynamical dark energy component with equation of state $w_{DE}(z)$ reads,

$$H(z) = H_0 [\Omega(z) + \Omega_{DE}(z)]^{1/2}, \quad (14)$$

in which $\Omega_{DE}(z)$ denotes the dark energy density fraction present in the Universe at redshift z and $\Omega(z)$ includes all the rest, that is, the density fraction of cold dark matter $\Omega_{cdm}(z)$ and of baryons $\Omega_b(z)$ in the case of the baseline, but also other ingredients available in extensions of it. From the dark energy conservation equation, the former can be written in terms of

the dark energy equation of state,

$$\Omega_{DE}(z) = \Omega_{DE} \exp \left(3 \int_0^z dz' \frac{1 + w_{DE}(z')}{(1 + z')} \right), \quad (15)$$

which, at low redshift where the dark energy is dominant, can be approximated by,

$$\Omega_{DE}(z \approx 0) \simeq \Omega_{DE} (1 + 3z \delta w_0), \quad (16)$$

where we wrote $w_{DE}(z \approx 0) \simeq -1 + \delta w_0$, with $|\delta w_0| \ll 1$ and constant, which is sensible enough for the present discussion. One can see that for the case of a phantom dark energy, such as the one featured by the RR model and for which $\delta w_0 < 0$, the predicted dark energy density $\Omega_{RR}(z)$ is generically smaller than Ω_Λ at $z \gtrsim 0$ and this explains why $H_{RR}(z)$ is lower compared to $H_\Lambda(z)$, for fixed parameter values. This is illustrated by the green line in the upper panel of Fig. 1, which shows the time evolution of the Hubble rate in the RR model for the cosmological parameters of the best-fitting Λ CDM model to the *Planck* dataset. Cosmological constraints on the RR model that are sensitive to $H(z)$ will then generically infer primarily higher values of H_0 , Ω_{cdm} , Ω_b , etc, for trying to compensate the change induced by the different dark energy modelling. Such a change does of course depend on the particular data set used into the constraints. We explore the case of the *Planck* CMB data into this subsection whereas we examine the SNIa *JLA* ones into the next one.

From the point of view of *Planck* CMB data, modifications to $H(z)$ at low redshift alter the predicted angular acoustic scale θ_* , which determines the position of the acoustic peaks of the CMB temperature power spectrum with a very good precision ($\lesssim 0.1\%$ at 1σ in the case of base Λ CDM) and is robust under cosmology change. The acoustic scale is defined

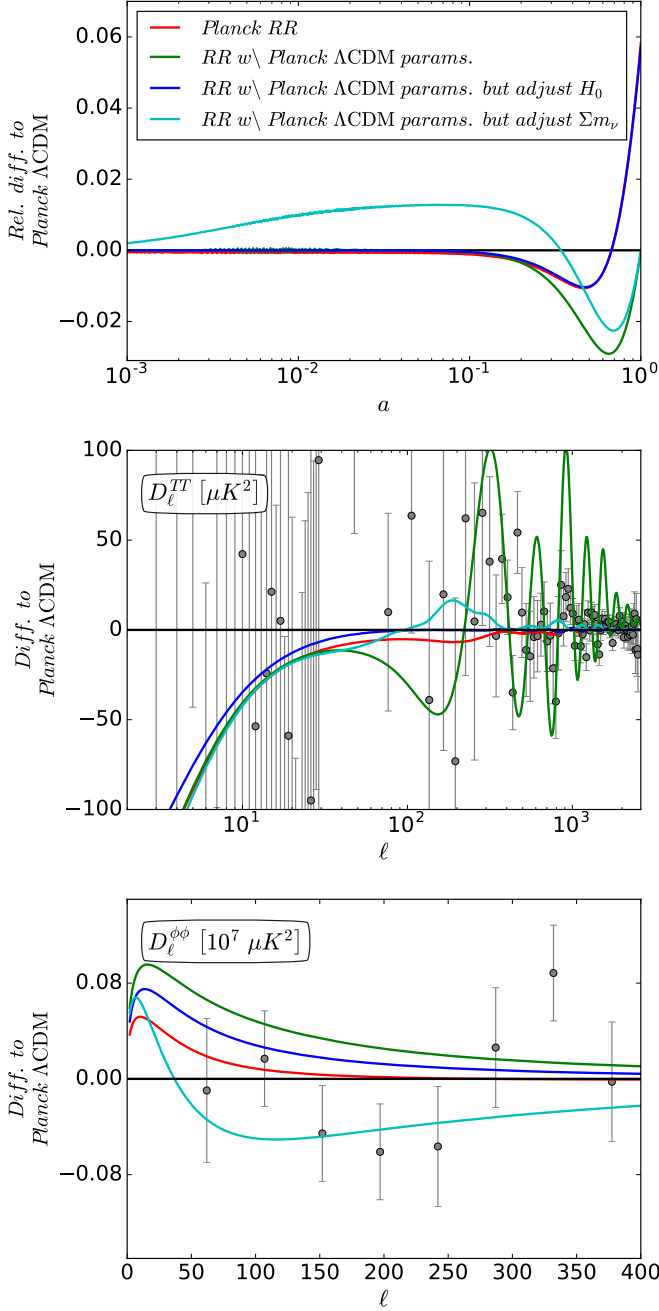


FIG. 1. Hubble expansion rate (top), CMB temperature power spectrum (middle) and CMB lensing power spectrum (bottom) for a few illustrative RR cosmologies, plotted as the relative difference to the best-fitting Λ CDM cosmology to the *Planck* dataset. The red curve displays the prediction of the best-fitting RR model to the *Planck* dataset. The green curves show the prediction of the RR gravity model with the same parameters as the best-fitting Λ CDM model to *Planck* data. The remainder curves show the same as the green ones, but with $H_0 = 71.31$ km/s/Mpc (blue) and $\sum m_\nu = 0.423$ eV (cyan), which have been adjusted to yield the same angular acoustic scale $\theta_* = 0.010414$ as Λ CDM. In the middle and lower panels, the grey symbols with errorbars show the power spectra as measured by the *Planck* satellite [59].

by $\theta_* \equiv r_*/D_A(z_*)$, with,

$$r_* \equiv \int_{z_*}^{\infty} \frac{c_s}{H(z)} dz, \quad (17)$$

$$D_A(z_*) \equiv \int_0^{z_*} \frac{dz}{H(z)}, \quad (18)$$

being respectively the sound horizon at the redshift of recombination z_* and the comoving angular diameter distance to recombination (the sound speed of the primordial plasma being $c_s = 1/\sqrt{3[1 + 3\Omega_b/(4\Omega_\gamma)]}$, where Ω_γ is the photon density). For fixed cosmological parameter values, r_* does not shift significantly from Λ CDM to RR because it is a function of early time background configurations and then does not depend on the particular dark energy modelling assumed here. At late time however, such a modelling becomes important and the lower expansion rate in the RR model leads to a larger $D_A(z_*)$, i.e. an object will span a smaller angle in the RR sky, which in turn lowers θ_* . The lower acoustic scale shifts the CMB temperature power spectrum towards higher multipoles ℓ , yielding the poor fit to the data seen in the middle panel of Fig. 1.

In the case of the *Planck* baseline, this discrepancy can be resolved in shifting either the background quantities H_0 , ω_b or ω_{cdm} (or equivalently Ω_b or Ω_{cdm}) present into $H(z)$. However, the shape information of the first CMB peaks such as the sound horizon, their relative position and their relative height provide strong, model-independent constraints on both ω_b and ω_{cdm} (see e.g. Refs. [94, 95]) and there is therefore only significant room for H_0 to vary. Consequently, since the dark energy featured by the RR model is phantom, H_0 is doomed to increase. The blue curves in Fig. 1 show the same as the green ones, but with H_0 adjusted to $H_0 = 71.31$ km/s/Mpc (whereas the RR bestfit is at $H_0 = 71.38$ km/s/Mpc) so as to yield the same θ_* as in the best-fitting Λ CDM model to *Planck*. This yields a cosmological scenario that is very similar to the best-fitting RR model to *Planck* (red curves in Fig. 1), whose goodness-of-fit to *Planck* is better than the base Λ CDM with $\Delta\chi^2 = 1.6$, mostly because of the lower power in the low- ℓ part of the CMB temperature power spectrum induced by a smaller ISW effect dominating at large-scales, as cosmic variance however. Such a preference being “inconclusive” according to the classification reported in our Table II both models are therefore statistically equivalent, given *Planck* 2015 CMB data.

2. BAPJ dataset

The observational performance of RR gravity however degrades when the model is confronted against the *BAPJ* dataset. The observational tensions that arise when one adds the BAO and SNIa data to the constraints are better illustrated in Fig. 2. The figure shows the 2d marginalized constraints on the H_0 - Ω_m plane for Λ CDM (upper panel) and RR (lower panel), obtained individually using the *Planck* dataset (red), SNIa data (grey) and BAO data (green). Contrary to Λ CDM, for the RR model the marginalized posterior suggests a $\sim 3-4\sigma$

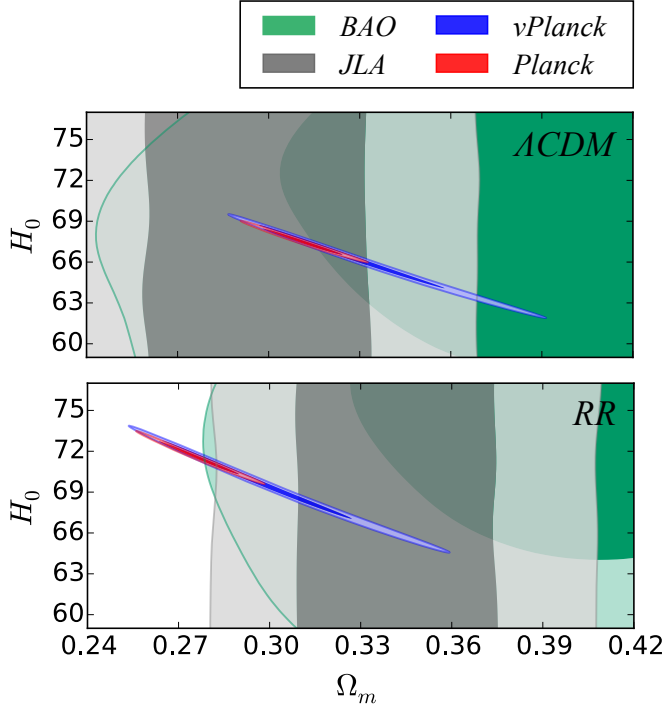


FIG. 2. Two dimensional marginalized constraints on the $H_0 - \Omega_m$ plane in the Λ CDM (top) and RR (bottom) models obtained with the *Planck* (red), BAO (green) and *JLA* (grey) datasets. The blue contours are the same as the red ones, but for constraints in which $\sum m_\nu$ is a free parameter. For fixed color, the two contour shades indicate 1σ and 2σ confidence level. The BAO and *JLA* contours do not change appreciably when $\sum m_\nu$ varies so we do not display them explicitly.

level tension between *Planck* and SNIa data. According to the above discussion, this can be understood in looking at the luminosity distance relevant for SNIa lightcurves,

$$D_L(z) \equiv (1+z) \int_0^z \frac{dz'}{H(z')}, \quad (19)$$

where the expression for $H(z)$ is found in Eq. (14). The latter measurements only constrain the total matter density Ω_m , whereas H_0 has been integrated out via marginalization on the absolute magnitude. Here the fact that the RR -dark energy is on the phantom side ($\delta w_0 < 0$ in Eq. (14) with Eq. (16)) has the net effect of raising Ω_m towards higher values in RR than in Λ CDM, for fixed luminosity distance. This shift has already been reported in [53] and is further illustrated by the grey contours in Fig. 2. We find $\Omega_m|_{\Lambda\text{CDM}} = 0.298 \pm 0.035$ and $\Omega_m|_{RR} = 0.343 \pm 0.033$, exhibiting a $\sim 1\sigma$ shift between both models, given SNIa *JLA* data.

This trend being inconsistent with the one inferred from *Planck*, this explains the origin of the dominant tension at $\Delta\chi^2 = 5.9$, which appears when constraining the RR model using joined *Planck* CMB and SNIa *JLA* data. Observe also that a discrepant CMB-BAO trend appears in RR compared to Λ CDM. It is however smaller compared to the CMB-SNIa one, and we therefore do not attempt to study it in more details.

B. Changing the prior: From RR to νRR

From the above discussion we have deduced that the late-time phantom nature of the RR effective dark energy induces an increase in H_0 given *Planck* CMB data, as this helps to resolve the mismatch with the CMB peaks position constraining θ_* . However, the same fact also induces an increase in Ω_m given SNIa data, which is inconsistent with *Planck*'s preference since the latter provides tight constraints on $\sim \Omega_m h^2$ which, together with an increase in H_0 , forces Ω_m to go down². This results in an overall dominant CMB-SNIa tension that renders the RR model non-concordant and disfavors it with respect to Λ CDM by $\Delta\chi^2 = 5.9$, given *BAPJ* data. Further, a posteriori constraints from RSD data have also been studied in Ref. [56] and the latter increase the overall tension even more, up to $\Delta\chi^2|_{\text{bapj}} + \Delta\chi^2|_{\text{rsd}}^{\text{post}} = 8.5$ ($\sim 3\sigma$) compared to Λ CDM, ruling out the nonlocal model given *BAPJ*+(post)*RSD* data.

This problem can be solved by considering extensions of the initial baseline, that is, not only changing the dark energy modellization as in Ref. [56], but also allowing other physically relevant parameters, otherwise fixed, to vary. Adding such an ingredient will open a new direction of the global parameter space and possibly provide an access to a new global maximum of the posterior probability distribution. The consequence of such a procedure is however the introduction of new degeneracies in the extended cosmological model coming together with a loss of constraining power for fixed data combination.

The extension we are looking for should consist in modifying the expansion history of the Universe at late-time in increasing the Hubble expansion rate at low redshift, $H(z \approx 0)$. It is therefore mostly related to the FLRW background cosmology and not to its linear perturbations. A natural candidate could have been to relax the assumption that the spatial curvature of the Universe vanishes $\Omega_K \neq 0$ since the latter redshifts as $(1+z)^2$. Such an hypothesis would imply the resulting Universe to be open. However such an assumption is beyond the scope of the present paper as, in addition to the cosmological constant paradigm, it would also attempt to refute the inflationary one.

As already mentioned here-above, a more sensible alternative is to allow the sum of the masses of active neutrino components to vary into the global fit. This is first because experimental constraints on $\sum m_\nu$ are very weak and there is no obvious reason why the latter needs to be fixed to $\sum m_\nu = 0.06 \text{ eV}$ on empirical grounds: this value only corresponds to the smallest mass-splitting measured by oscillations experiments (see subsection IV F for more details and references). Second, and regarding our problem, a boost in neutrino masses can effectively preserve the expansion rate at

² This behavior is a generic one for reasonably smooth phantom dark energy as indicated by the degenerate directions in the $\Omega_m - w_0$ plan while constraining w_0 CDM models given equivalent CMB and SNIa data as those used in this work (see e.g. Fig. 16 of Ref. [85]).

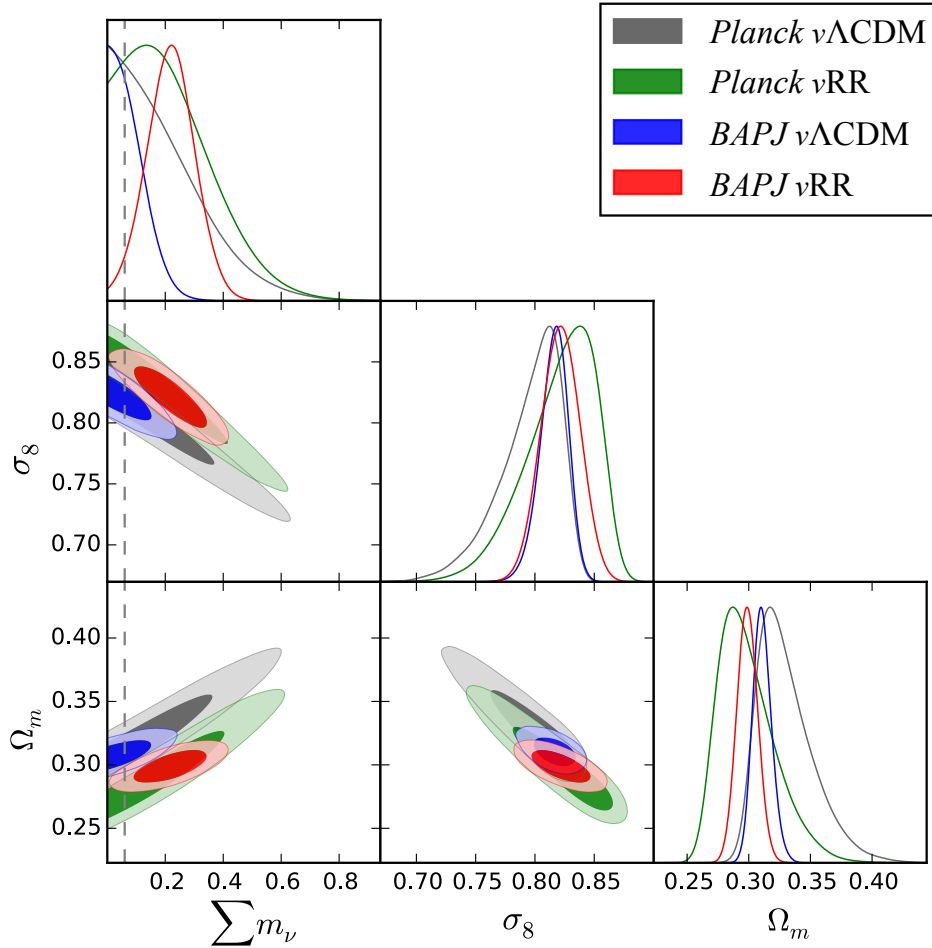


FIG. 3. One and two dimensional marginalized constraints on the parameters $\sum m_\nu$, σ_8 and Ω_m in the νRR and $\nu\Lambda CDM$ models, obtained with the *Planck* and *BAPJ* datasets, as labelled. For fixed color, the two contour shades indicate 1σ and 2σ limits.

early times if the neutrinos are still relativistic at photon decoupling, so as CMB anisotropies remain unaffected, and still raise the energy density of pressureless matter (after they turn non-relativistic), which therefore increases the expansion rate during the matter era. And third, the free-streaming behavior exhibited by a more massive neutrino component helps to tame the growth rate of structures and therefore potentially lowers the additional discrepancy caused in including RSD data (see Ref. [96] for a detailed analysis of the effects induced by massive neutrinos on cosmological observables). Thus, we can expect that the RR model would prefer a higher value of $\sum m_\nu$ than 0.06 eV and that the CMB-SNIa tension ruling it out disappears on the new best-fit. This is what is discussed in more details in the following.

The cyan curves in Fig. 1 effectively illustrate such facts in showing the same as the blue curves, but instead of adjusting H_0 to give the same θ_* as in ΛCDM , one adjusts the neutrino masses to $\sum m_\nu = 0.42$ eV. The middle panel of Fig. 1 also confirms that this would help to drastically improve the goodness-of-fit to *Planck* data compared to the RR model on the ΛCDM best-fitting parameters. This is a clear hint that the degenerate effects of H_0 , $\sum m_\nu$ and a late-time phantom dark

energy on θ_* can therefore be exploited to try to reconcile the *Planck* CMB and SNIa *JLA* constraints given the RR nonlocal gravity.

The results of Bayesian parameter inference for the extended $\nu\Lambda CDM$ and νRR models are presented in Table II and can be compared to the ones of ΛCDM and RR given *Planck* and *BAPJ* data. A triangle plot including selected parameters is shown in Fig. 3.

Figure 2 illustrates better the beneficial impact of varying $\sum m_\nu$ in the constraints given RR -dark energy compared to Λ . The blue contours show the *Planck* constraints on the $H_0 - \Omega_m$ plane when $\sum m_\nu$ is a free parameter (quoted $\nu Planck$ for definiteness). For the nonlocal gravity model, the latter is now overlapping the corresponding SNIa one, weakening the CMB-SNIa tension as witnessed by the corresponding individual $\Delta\chi^2$ values reported in Table II.

A remarkable aspect of the combination of the CMB, SNIa and BAO data in the constraints given RR nonlocal gravity is the evidence for non-vanishing neutrino masses. Figure 3, shows that $\sum m_\nu > 0$ at $\sim 2\sigma$ level, with the best-fitting value being $\sum m_\nu \approx 0.21$ eV. As depicted above, such a shift is primarily caused by the relatively smooth, late-time

and phantom nature featured by the effective dark energy described by the RR nonlocal model. These constraints are very different than in $\nu\Lambda$ CDM for which the data only sets an upper bound on $\sum m_\nu$. In the following, we will see that such a preference of the $\nu\Lambda$ CDM model for lower values of $\sum m_\nu$ reflects one of its weakness in a Bayesian model comparison context, and therefore opens room for alternative dark energy models including a wider prior on $\sum m_\nu$ to compete with it.

C. Bayesian model comparison

In the following, we compare the $\nu\Lambda$ CDM and νRR models against each other in computing the associated Bayes factor $B_{\nu\Lambda, \nu RR}$ and compare it with the Bayesian Information Criterion (BIC)³ differences that are reported in Table I. Degrees of significance used in this work are reported in Table II for definiteness of the discussion, while a Bayes factor B_{01} comparing model \mathcal{M}_0 against model \mathcal{M}_1 can always be thought of as telling betting odds of $B_{01} : 1$ in favor of the former given the data.

For computing $B_{\nu\Lambda, \nu RR}$ we use a combination of statistical coherence and the Savage-Dickey density ratio (SDDR) (see Ref. [56] and references therein for details) that exploits the nested structure of the overall models discussed in that work. This allows one to get the latter in a rather economic way in writing,

$$B_{\nu\Lambda, \nu RR} \equiv \frac{P(d|\mathcal{M}_{\nu\Lambda})}{P(d|\mathcal{M}_{\nu RR})} \quad (21)$$

$$= \frac{P(d|\mathcal{M}_{\nu\Lambda})}{P(d|\mathcal{M}_\Lambda)} \frac{P(d|\mathcal{M}_\Lambda)}{P(d|\mathcal{M}_{RR})} \frac{P(d|\mathcal{M}_{RR})}{P(d|\mathcal{M}_{\nu RR})} \quad (22)$$

$$= \frac{B_{RR, \nu RR}}{B_{\Lambda, \nu\Lambda}} B_{\Lambda, RR}, \quad (23)$$

where $P(d|\mathcal{M}_i)$ is the marginal likelihood (evidence) of the data d given the model \mathcal{M}_i . The factor $B_{\Lambda, RR}$ appearing above is one of the main results of Ref. [56] and has been computed to be $B_{\Lambda, RR} = 22.7$. The remaining factors are computed for the model $i = \Lambda, RR$ through the SDDR,

$$B_{i, \nu i} = \frac{P(\sum m_\nu = 0.06 | d, \mathcal{M}_{\nu i})}{P(\sum m_\nu = 0.06 | \mathcal{M}_{\nu i})}, \quad (24)$$

and since we chose the same prior for both $\nu\Lambda$ CDM and νRR parameter spaces (in particular on $\sum m_\nu$) the contribution of

³ The Bayesian Information Criterion is given by (see e.g. Ref. [52] for more details),

$$\text{BIC} \equiv \chi^2 + k \ln N, \quad (20)$$

where k is the number of parameters and N the number of data points. The lower the BIC the better the model. Since these parameters are equal within the models that we compare throughout this work, we can therefore only use the difference between the models χ^2 as a BIC diagnostic. The latter criterion originates from an approximation of the Bayesian evidence assuming gaussianity of the posterior, a likelihood dominated regime and weak correlations between parameters.

the latter simplifies. Eq. (23) then yields,

$$B_{\nu\Lambda, \nu RR} = \frac{P(\sum m_\nu = 0.06 | d, \mathcal{M}_{\nu RR})}{P(\sum m_\nu = 0.06 | d, \mathcal{M}_{\nu\Lambda})} B_{\Lambda, RR}, \quad (25)$$

and we find,

$$B_{\nu\Lambda, \nu RR} = \frac{1}{12.5} \times 22.7 = 1.8 = e^{0.6}, \quad (26)$$

which is one of the main results of this article. It tells that νRR is statistically equivalent to the $\nu\Lambda$ CDM with odds of 1.8 : 1 for the latter, instead of being “moderate-to-strongly” disfavored in the non- ν case with 22.7 : 1, given $BAPJ$ data. It is invariant under prior changes on $\sum m_\nu$ (as long as they are assumed to be equal) and leads to several implications. This result shows that allowing $\sum m_\nu$ to vary within $[0, 5]$ eV helps to reconcile RR -gravity with the data as already noticed above, but it also has the effect of handicapping the Λ CDM cosmology. This can be seen through the fact that the BIC difference applied to comparing $\nu\Lambda$ CDM against νRR given $BAPJ$ leads to biased results. Indeed in comparing the shifts endured by the results of both methods in varying $\sum m_\nu$,

$$\text{BIC} : \Delta\chi^2|_{\Lambda, RR} = 5.9 \rightarrow \Delta\chi^2|_{\nu\Lambda, \nu RR} = 3.4, \quad (27)$$

$$\text{Bayes} : \ln B_{\Lambda, RR} = 3.1 \rightarrow \ln B_{\nu\Lambda, \nu RR} = 0.6, \quad (28)$$

where all are in favor of Λ given $BAPJ$ data, and referring to Table II, one can see a significant discrepancy between the results from the BIC differences and Bayes factors. While the former announces a reduction from “weak”/“moderate-to-strong” only to “weak” evidence in favor of $\nu\Lambda$ CDM, Bayesian model comparison tells that the latter “moderate-to-strong” evidence is in fact comfortably reduced to an “inconclusive” one. Obviously one should trust the result of Eq. (28) since the one of Eq. (27) is actually obtained through an approximation of it. It is because, beside of the net maximum likelihood shift encapsulated in $\Delta\chi^2$ favoring the RR model, Occam’s razor further penalizes the $\nu\Lambda$ CDM one.

In what follows, we address a rough analysis for trying to understand to which extent allowing the absolute neutrino mass to vary is beneficial for RR -dark energy, given $BAPJ$ data. Coming back to Eq. (24), in our present context we can write,

$$B_{i, \nu i} = \frac{P(\sum m_\nu = 0.06 | d, \mathcal{M}_{\nu i})}{P(\sum m_\nu = 0.06 | \mathcal{M}_{\nu i})} = \frac{L_i}{V_i} P_i, \quad (29)$$

where L_i is the value of the marginalized 1d posterior for $\sum m_\nu$ (normalized to its maximum) at the nesting point, V_i is the volume of it and P_i is the upper bound of the prior on the sum of the neutrino masses, $\sum m_\nu \in [0, P_i]$. We find,

$$L_{RR} = 0.19, \quad V_{RR} = 0.2, \quad (30)$$

$$L_\Lambda = 1.0, \quad V_\Lambda = 0.08, \quad (31)$$

where we have set $P_i = 5$ in either cases. One can then compute,

$$B_{\Lambda, \nu\Lambda} = 12.5 \times 5 = 62.5, \quad B_{RR, \nu RR} = 1 \times 5, \quad (32)$$

TABLE II. Scale used for comparing model \mathcal{M}_1 against model \mathcal{M}_0 in this article, i.e. for interpreting their BIC difference $\Delta\chi^2_{01} \equiv \chi^2_1 - \chi^2_0$ and their log-Bayes factors $\ln B_{01}$. Positivity of the latter tends to favor \mathcal{M}_0 . These scales are taken as a rule of thumb inspired by Secs. 2.6-2.10 of Ref. [97] in accordance with the (more conservative) Jeffreys' scale of Ref. [52] (see also Ref. [98] for a comparison of the latter with the original scale proposed by Jeffreys).

Interpretation	$\Delta\chi^2$	$\ln B_{01}$
"inconclusive"	0–2	0–1
"weak"	2–6	1–2.5
"moderate-to-strong"	6–10	2.5–5
"strong"	> 10	> 5

which in particular shows that the Λ -based model provides “moderate-to-strong” evidence with odds of 62:1 for fixing $\sum m_\nu = 0.06$ eV. Although the latter has a non-negligible contribution coming from the prior, it also has a non-negligible likelihood one (essentially originating from boundary effects) which is a handicap when compared against models preferring higher neutrino masses such as the nonlocal one studied in this work. As can be seen from Fig. 3, this is because the Λ CDM marginalized posterior on $\sum m_\nu$ hits the lower bound of the prior at 0.06 eV, which involves a loss of posterior volume and a waste of prior one. In the RR case the situation is different since the latter prefers non-vanishing neutrino masses at 2σ level, and exploits therefore better the $BAPJ$ data. This contributes to Occam’s razor effect intrinsically taken into account in Bayesian model comparison and partially explains why the RR nonlocal model undergoes a favorable and significant change when compared against Λ CDM after allowing $\sum m_\nu$ to vary (Eq. (28)). Moreover, this also explains why the BIC difference effectively fails when comparing $\nu\Lambda$ CDM against νRR given $BAPJ$ data, because the latter is only sensitive to the maximum of the posteriors, not to their entire volume.

The RR nonlocal model described by the action (1) is therefore statistically equivalent to Einstein gravity supplemented by a cosmological constant when reconsidering the prior on the neutrino sector, that is changing the cosmological parametrization from (11) to (13), given $BAPJ$ data. This has been made possible in exploiting an apparent degeneracy at the background level between H_0 , $\sum m_\nu$ and the nature of the effective dark energy described by the nonlocal model, which was illustrated in Fig. 2. Such a fact motivates the use of additional data, in particular coming from galaxy redshift surveys, for being able to make a distinction between the $\nu\Lambda$ CDM and the νRR cosmological models and we provide an outlook to such a task in what follows.

D. Post constraints from Redshift-Space Distortions data

Apart from secondary CMB anisotropies such as ISW or lensing effects, $\sum m_\nu$ mostly finds its constraints from background-geometrical features through the $BAPJ$ dataset. However, massive neutrinos give rise to characteristic inho-

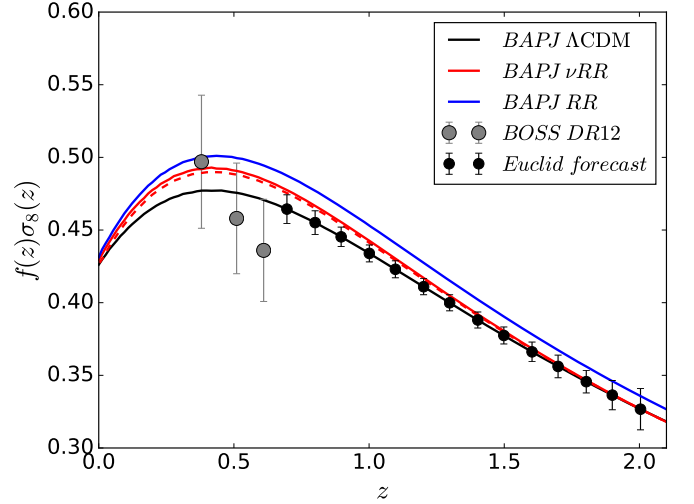


FIG. 4. Time evolution of the growth rate $f\sigma_8$ for the best-fitting Λ CDM, RR and νRR models to the $BAPJ$ dataset. For the case of the νRR model (red), the solid and dashed lines display the result at $k = 0.01$ h/Mpc and $k = 0.5$ h/Mpc, respectively. For the Λ CDM and RR models the growth rate is scale-independent (apart from the very small scale-dependency induced by the small neutrino fraction, $\sum m_\nu = 0.06$ eV). The grey symbols show the observational determination from the final BOSS DR12 release [99]. The black symbols show the forecasted precision for Euclid, centered around the Λ CDM result.

mogeneous and anisotropic signatures induced by their thermal velocity flow, in particular, they do not cluster as strongly as cold dark matter inside regions delimited by their free-streaming scale and source anisotropic stresses. Below their free-streaming scale, the neutrino perturbations are smoothed out and this causes a suppression of the late-time matter power spectrum at mid-to-small cosmological scales, a decrease of the lensing power and of the growth of structures in a scale-dependent manner within the linear regime [100, 101], as well as non-linear effects [102, 103]. Additional data putting stronger constraints on these features are therefore relevant to include into the global fit. Nevertheless, the presence of an appreciable fraction of massive neutrinos can have partial degenerate effects with a positive fifth force present in modified gravity scenarios. Such a fifth force being present at late-times in the RR model, it was found in Refs. [54, 56] that it enhances the growth of linear and non-linear structures compared to the one described by Λ CDM. Into the latter reference, this was quantified by a BIC of $\Delta\chi^2 = 2.6$ in favor of Λ CDM given RSD data. In this part, we study the impact of a massive neutrino component on the linear growth rate of structure modelled by $f\sigma_8$ using the same method, in particular, taking the amplitude of the linear matter power spectrum set on the $BAPJ$ bestfit.

The degenerate effects present between a massive neutrino fraction and growth are well-illustrated at linear level from the degeneracy direction observed in the $\sigma_8 - \sum m_\nu$ plane in Fig. 3, both are anti-correlated: the higher the massive neutrino fraction $\Omega_\nu \sim \sum m_\nu$, the lower σ_8 . Given *Planck* data, the mean value inferred on σ_8 for Λ CDM is smaller than the

one provided by RR , witnessing the higher growth within the nonlocal model, and their mean values are generically smaller in the ν -extended case. For CMB only, we find that the departure of the best-fit value of $\sum m_\nu$ from the lower bound of the prior in RR cosmology is caused by the addition of the external *Planck* CMB lensing power spectrum which is sensitive to a weighted projection of density fluctuations along the line-of-sight. Joining BAO+SN Ia data then pulls the total matter density fraction Ω_m to higher values, involving a stronger increase in the absolute neutrino mass that preserves the value of σ_8 close to the one inferred in Λ CDM. Focusing on the growth, Fig. 4 shows the time evolution of $f\sigma_8$ for the best-fitting Λ CDM, RR and νRR models to the *BAPJ* dataset and, as anticipated, the growth rate is lower in νRR compared to the RR model. The figure also displays the most recent observational determinations of $f\sigma_8$ from the DR12 BOSS analysis [99] (grey symbols with errorbars). Using these data, the reduced χ^2_{red} values for the Λ CDM, RR and νRR models are, respectively⁴, $\chi^2_{\text{red}} = 0.58$, $\chi^2_{\text{red}} = 1.38$ and $\chi^2_{\text{red}} = 0.97$. More pragmatically for comparison with the previous results of Ref. [56], we compute the corresponding χ^2 values using the same data points as in the latter, that is, the ones collected from 6dF GRS [104] at $f\sigma_8(0.067) = 0.423 \pm 0.055$, SDSS LRG [105] at $f\sigma_8(0.3) = 0.49 \pm 0.08$, SDSS MGS [106] at $f\sigma_8(0.15) = 0.63^{+0.027}_{-0.24}$, BOSS LOWZ [107] at $f\sigma_8(0.32) = 0.371 \pm 0.091$, BOSS CMASS [108] at $f\sigma_8(0.57) = 0.441 \pm 0.0434$ ⁵, WiggleZ [109] at $f\sigma_8(0.44) = 0.413 \pm 0.08$, $f\sigma_8(0.6) = 0.39 \pm 0.063$, $f\sigma_8(0.73) = 0.437 \pm 0.072$ and VIPERS [110] at $f\sigma_8(0.8) = 0.47 \pm 0.08$. The corresponding goodness-of-fit read,

$$\chi^2_{\Lambda\text{CDM}} = 3.9, \quad \chi^2_{RR} = 6.5, \quad \chi^2_{\nu RR} = 5.2, \quad (33)$$

which shows that the fit is indeed improved in going from RR to νRR with BIC values changing from $\Delta\chi^2 = 2.6$ to $\Delta\chi^2 = 1.3$ in favor of Λ CDM. Therefore, we can conclude that providing to $\sum m_\nu$ a more reasonable prior range helps to decrease the discrepancy of the RR nonlocal gravity model with growth rate measurements and brings down the total discrepancy from $\Delta\chi^2|_{\text{bapj}} + \Delta\chi^2|_{\text{rsd}}^{\text{post}} = 8.5$ ($\sim 3\sigma$) to $\Delta\chi^2|_{\text{bapj}} + \Delta\chi^2|_{\text{rsd}}^{\text{post}} = 4.6$ ($\sim 2\sigma$) given *BAPJ*+(post)*RSD*, which induces a significant change in the (although approximated) statistical conclusion.

In turn, this shows that the data considered in this work do not possess enough constraining power to clearly distinguish between Λ CDM and RR cosmologies. Nevertheless, the situation is expected to be different in a survey like *Euclid* [111]. This is illustrated by the black symbols in Fig. 4, which show an estimate of the forecast errorbars for this future mission (taken from Fig. 3 of Ref. [112]), centred around the Λ CDM

prediction. One notes that the difference between Λ CDM and νRR is larger than the forecast precision of *Euclid* for $z < 1$, from which we can conclude that, despite partial degeneracies between the effects of massive neutrinos and the RR -modifications to gravity, there is still room for future $f\sigma_8$ data to be used to help distinguishing between Λ CDM and RR cosmologies. Of course, our results presented here are only presenting generic trends and a more thorough analysis would consist in including peculiar velocity measurements into the global fit, as these are degenerated with geometric distortions longitudinal and transverse to the light-of-sight induced by the Hubble flow (see e.g. [63] where such more complete *Euclid*-like likelihoods were exploited). Further constraints from weak lensing observations such as those of CFHTLenS [113] or KiDS [114], providing alternatives to *Planck* CMB lensing data, also prove to be of particular interest for constraining the ν -extended models. Indeed, the latter also constrain the nature of the dark energy and, although to a smaller extent, the absolute neutrino mass as well [115]. Such an analysis is left for future work.

As a final remark, a larger fraction of massive neutrinos in cosmological models contributes to an increased scale-dependence in the linear growth of structure. This may raise some concerns when confronting models like the best-fitting νRR model to *BAPJ* against $f\sigma_8$ values, because the latter is usually extracted from galaxy survey data using RSD models assuming the growth to be scale-independent (see e.g. Ref. [116] for an exception to this fact and Ref. [117] for a validation study of RSD modelling in DGP gravity which exhibits scale-independent linear growth). If the scale-dependence in the νRR is non-negligible compared to the precision targeted, extra care is required in the analysis of the data before observational constraints can be performed. To test such a fact, we plot in Fig. 4 the evolution of $f\sigma_8$ in the νRR model for $k = 0.01$ h/Mpc (red solid) and $k = 0.5$ h/Mpc (red dashed). One notes that the k -dependence is small compared to the expected precision of *Euclid*, which suggests that standard methods can be used to constrain the νRR model.

E. A word on H_0

Another interesting outcome of the constraints on the RR model relates to the preferred values of H_0 . For the best-fitting Λ CDM model to the *BAPJ* dataset, one finds $H_0 = 67.67 \pm 0.50$ km/s/Mpc (cf. Table I), which lies $\sim 1\sigma$ below the determination from local measurements discussed in Ref. [118], which sets $H_0 = 70.6 \pm 3.3$ km/s/Mpc. More recently, the work of Ref. [119] sets a higher value $H_0 = 73.24 \pm 1.74$ km/s/Mpc (see also Refs. [120, 121]). Further, recent determinations of H_0 using hyperparameters, $H_0 = 73.75 \pm 2.11$ km/s/Mpc [122] or from gravitational lensing time delay methods, $H_0 = 71.9^{+2.4}_{-3.0}$ km/s/Mpc [123], are also significantly away from Λ CDM.

The seriousness of the above-mentioned H_0 tensions is still subject to current debates and one still needs to understand better the role of systematics before claiming the need of new physics (see e.g. Refs. [124, 125]). Nevertheless, tak-

⁴ These values do not consider the mid-redshift data point. This is because the associated galaxy sample completely overlaps with those of the other two points, which can therefore be treated as independent. The number of degrees of freedom is therefore two.

⁵ Replacing the latter BOSS data by those of Ref. [99] does not significantly affect our statistical conclusions.

ing the current measurements at face value, one notes that for the best-fitting νRR model to the *BAPJ* dataset one has $H_0 = 69.49 \pm 0.8$, which significantly ameliorates the agreement with the local determinations and would therefore improve further the global fit.

F. The importance of terrestrial determinations of $\sum m_\nu$

Beside cosmological probes, there are solar, atmospheric and reactor experiments that are able to set constraints on $\sum m_\nu$ as well and these are completely independent of any cosmological modelling assumption. The lower bounds on $\sum m_\nu$ come from neutrino oscillations experiments which, assuming a massless eigenstate, set $\sum m_\nu > 0.05$ eV and $\sum m_\nu > 0.1$ eV for normal and inverted mass hierarchies respectively (the value of $\sum m_\nu > 0.06$ eV chosen into the *Planck* baseline corresponds to the result of an anterior global fit performed in Ref. [126] for a normal hierarchy). The current best upper bounds are obtained by analysing the high-energy part of the spectrum of Tritium β -decay in experiments such as MAINZ and TROITSK and set the electron neutrino mass to $m_{\nu_e} \lesssim 2.2$ eV (2σ) which corresponds to $\sum m_\nu \lesssim 6.6$ eV in our context. Future Tritium β -decay experiments such as KATRIN will be sensitive to mass scales $\sum m_\nu \lesssim 0.6$ eV at 90% confidence level. The sensitivity can be even better if neutrinos turn out to be Majorana particles, in which case neutrinoless double β decay experiments should be able to probe the region corresponding to $\sum m_\nu \gtrsim 0.3$ eV with high precision (see e.g. Refs. [127, 128] for reviews). These forecast sensitivities can therefore be proven to be useful for complementing cosmological observations and for discriminating between competing cosmological scenarios such as Λ CDM and RR gravity.

V. SUMMARY & CONCLUSION

We have revisited the observational constraints of Ref. [56] where the nonlocal model of modified gravity described by the action (1) was found to be disfavored against Λ CDM with odds of 22 : 1, given CMB+SN Ia+BAO data whose details are found in Sec. III of the present work. Such a result was mostly caused by a CMB-SN Ia tension in the $\Omega_m - H_0$ plane that we analyzed in more details into our Sec. IV. We have found that the discrepancy was mostly caused by the quite smooth, late-time and phantom nature of the effective dark energy described by the nonlocal model, because of the decrease it induces on the late-time Hubble expansion rate compared to that described by Λ CDM. Such a fact generically implies a smaller acoustic scale θ_* for the CMB which is corrected by the inference of a higher value of H_0 given the nonlocal model, as well as a larger luminosity distance for SN Ia that is compensated by a larger Ω_m . The shape information from CMB temperature power spectrum constraining well ω_m , which is a multiplicative combination of both, such trends are contradictory as illustrated in Fig. 2.

We have then shown that in changing the prior on the neutrino sector from one dominant massive neutrino species of fixed mass to three degenerated ones, with a larger prior interval on their absolute mass, resolved the tension. The ν -extended nonlocal gravity model, denoted νRR here-above, ends up to be statistically equivalent to $\nu\Lambda$ CDM given CMB+SN Ia+BAO with odds of 1.8 : 1 in favor of the latter. We have shown that this was caused by a better fit of the nonlocal model to the data, but also by volume effects induced by the preference of the Λ CDM model for small absolute neutrino masses, intrinsically penalizing it on Bayesian statistical grounds. As a result, the absolute neutrino mass is inferred to be non-zero $\sum m_\nu > 0$ at $\sim 2\sigma$ level, with the best-fitting value being $\sum m_\nu \approx 0.21$ eV, showing explicitly that $\sum m_\nu$ is cosmological model-dependent. We have then placed constraints from RSD data a posteriori on both models, i.e. once the respective matter power spectra have been set on the CMB+SN Ia+BAO bestfit, which have been shown to be improved as well by the presence of a higher neutrino fraction Ω_ν into the nonlocal cosmology. Further constraints from local measurements of H_0 were also discussed as these are favorable to the nonlocal gravity model inferring a value of $H_0 = 69.49 \pm 0.8$ which is $\sim 2\sigma$ above $H_0 = 67.67 \pm 0.5$, inferred from Λ CDM.

In conclusion, changing the prior into the neutrino sector allowed the RR nonlocal gravity model to fit current CMB+SN Ia+BAO data as well as Λ CDM, providing different constraints on the absolute neutrino mass $\sum m_\nu$, and also improved the fit to RSD data a posteriori done. Such a fact reveals that the degenerate effects between modifications to gravity and massive neutrinos are not only present in theories where gravity is modified locally, as already pointed out into the literature, but can also exist in theories that modify gravity nonlocally. In turn, this further suggests that a more sensible model to choose for competing against modified gravity ones equitably is the ν -extended version of Λ CDM that we denoted $\nu\Lambda$ CDM, not Λ CDM itself. Furthermore, our study also motivates the use of additional data coming from galaxy redshift surveys for being able to discriminate between these models and we have provided an illustration to this in considering forecast constraints from *Euclid* RSD data. In conjunction with complementary data from other cosmological observations and terrestrial neutrino experiments, these can provide tighter constraints on the absolute neutrino mass, whose fundamental origin still remains unknown.

ACKNOWLEDGMENTS

The author sincerely thanks Alexandre Barreira for his useful contributions to early stages of this work and for fruitful discussions. Many thanks to Martin Kunz and Michele Maggiore for their useful comments about the manuscript and to Leila Haegel for sharing her expertise in experimental neutrino research. Numerical work presented in this publication used the Baobab cluster of the University of Geneva. YD is supported by the Fonds National Suisse.

-
- [1] C. M. Will, Living Rev. Rel. **17**, 4 (2014), arXiv:1403.7377 [gr-qc].
- [2] A. G. Riess *et al.* (Supernova Search Team), Astron. J. **116**, 1009 (1998), arXiv:astro-ph/9805201 [astro-ph].
- [3] S. Perlmutter *et al.* (Supernova Cosmology Project), Astrophys. J. **517**, 565 (1999), arXiv:astro-ph/9812133 [astro-ph].
- [4] A. R. Liddle and D. H. Lyth, Phys. Rept. **231**, 1 (1993), arXiv:astro-ph/9303019 [astro-ph].
- [5] S. M. Carroll, *The new cosmology. Proceedings, Conference on Strings and Cosmology, College Station, USA, March 14-17, 2004, and Mitchell Symposium on Observational Cosmology, College Station, USA, April 12-16, 2004*, eConf **C0307282**, TTH09 (2003), [AIP Conf. Proc.743,16(2005)], arXiv:astro-ph/0310342 [astro-ph].
- [6] E. Bianchi and C. Rovelli, (2010), arXiv:1002.3966 [astro-ph.CO].
- [7] T. Clifton, P. G. Ferreira, A. Padilla, and C. Skordis, Phys. Rept. **513**, 1 (2012), arXiv:1106.2476 [astro-ph.CO].
- [8] A. Joyce, B. Jain, J. Khoury, and M. Trodden, Phys. Rept. **568**, 1 (2015), arXiv:1407.0059 [astro-ph.CO].
- [9] E. Berti *et al.*, Class. Quant. Grav. **32**, 243001 (2015), arXiv:1501.07274 [gr-qc].
- [10] K. Koyama, Rept. Prog. Phys. **79**, 046902 (2016), arXiv:1504.04623 [astro-ph.CO].
- [11] D. Lovelock, J. Math. Phys. **12**, 498 (1971).
- [12] D. Lovelock, J. Math. Phys. **13**, 874 (1972).
- [13] K. S. Stelle, Gen. Rel. Grav. **9**, 353 (1978).
- [14] G. Dvali, G. Gabadadze, and M. Porrati, Physics Letters B **485**, 208 (2000), hep-th/0005016.
- [15] J. W. Moffat, JCAP **0603**, 004 (2006), arXiv:gr-qc/0506021 [gr-qc].
- [16] C. de Rham and G. Gabadadze, Phys. Rev. **D82**, 044020 (2010), arXiv:1007.0443 [hep-th].
- [17] C. de Rham, G. Gabadadze, and A. J. Tolley, Phys. Rev. Lett. **106**, 231101 (2011), arXiv:1011.1232 [hep-th].
- [18] S. F. Hassan and R. A. Rosen, JHEP **02**, 126 (2012), arXiv:1109.3515 [hep-th].
- [19] K. Hinterbichler and R. A. Rosen, JHEP **07**, 047 (2012), arXiv:1203.5783 [hep-th].
- [20] C. de Rham, Living Rev. Rel. **17**, 7 (2014), arXiv:1401.4173 [hep-th].
- [21] J. Gleyzes, D. Langlois, F. Piazza, and F. Vernizzi, JCAP **1308**, 025 (2013), arXiv:1304.4840 [hep-th].
- [22] J. Gleyzes, D. Langlois, and F. Vernizzi, Int. J. Mod. Phys. **D23**, 1443010 (2015), arXiv:1411.3712 [hep-th].
- [23] A. O. Barvinsky and G. A. Vilkovisky, Nuclear Physics B **282**, 163 (1987).
- [24] A. O. Barvinsky and G. A. Vilkovisky, Nuclear Physics B **333**, 471 (1990).
- [25] E. V. Gorbar and I. L. Shapiro, JHEP **02**, 021 (2003), arXiv:hep-ph/0210388 [hep-ph].
- [26] I. Antoniadis and E. Mottola, Phys. Rev. **D45**, 2013 (1992).
- [27] A. O. Barvinsky, Y. V. Gusev, G. A. Vilkovisky, and V. V. Zhytnikov, Nucl. Phys. **B439**, 561 (1995), arXiv:hep-th/9404187 [hep-th].
- [28] N. Arkani-Hamed, S. Dimopoulos, G. Dvali, and G. Gabadadze, (2002), arXiv:hep-th/0209227 [hep-th].
- [29] A. O. Barvinsky, Phys. Lett. **B572**, 109 (2003), arXiv:hep-th/0304229 [hep-th].
- [30] H. W. Hamber and R. M. Williams, Phys. Rev. **D72**, 044026 (2005), arXiv:hep-th/0507017 [hep-th].
- [31] D. Lopez Nacir and F. D. Mazzitelli, Phys. Rev. **D75**, 024003 (2007), arXiv:hep-th/0610031 [hep-th].
- [32] A. O. Barvinsky, Phys. Lett. **B710**, 12 (2012), arXiv:1107.1463 [hep-th].
- [33] T. Biswas, E. Gerwick, T. Koivisto, and A. Mazumdar, Physical Review Letters **108**, 031101 (2012), arXiv:1110.5249 [gr-qc].
- [34] L. Modesto, Phys. Rev. D **86**, 044005 (2012), arXiv:1107.2403 [hep-th].
- [35] T. Biswas, A. Mazumdar, and W. Siegel, JCAP **0603**, 009 (2006), arXiv:hep-th/0508194 [hep-th].
- [36] G. Calcagni and L. Modesto, Phys. Rev. D **91**, 124059 (2015), arXiv:1404.2137 [hep-th].
- [37] C. Wetterich, Gen. Rel. Grav. **30**, 159 (1998), arXiv:gr-qc/9704052 [gr-qc].
- [38] C. Espriu, T. Multamaki, and E. Vagenas, Physics Letters B **628**, 197 (2005).
- [39] S. Nojiri and S. D. Odintsov, Phys. Lett. **B659**, 821 (2008), arXiv:0708.0924 [hep-th].
- [40] S. Deser and R. P. Woodard, Phys. Rev. Lett. **99**, 111301 (2007), arXiv:0706.2151 [astro-ph].
- [41] T. Koivisto, Phys. Rev. **D77**, 123513 (2008), arXiv:0803.3399 [gr-qc].
- [42] S. Deser and R. Woodard, JCAP **1311**, 036 (2013), arXiv:1307.6639 [astro-ph.CO].
- [43] M. Maggiore, Phys. Rev. **D89**, 043008 (2014), arXiv:1307.3898 [hep-th].
- [44] P. G. Ferreira and A. L. Maroto, Phys. Rev. **D88**, 123502 (2013), arXiv:1310.1238 [astro-ph.CO].
- [45] M. Maggiore and M. Mancarella, Phys. Rev. **D90**, 023005 (2014), arXiv:1402.0448 [hep-th].
- [46] E. Mitsou, *Aspects of Infrared Non-local Modifications of General Relativity*, Ph.D. thesis, Geneva U. (2015), arXiv:1504.04050 [gr-qc].
- [47] G. Cusin, S. Foffa, M. Maggiore, and M. Mancarella, Phys. Rev. **D93**, 043006 (2016), arXiv:1512.06373 [hep-th].
- [48] G. Cusin, S. Foffa, M. Maggiore, and M. Mancarella, Phys. Rev. **D93**, 083008 (2016), arXiv:1602.01078 [hep-th].
- [49] H. Nersisyan, Y. Akrami, L. Amendola, T. S. Koivisto, J. Rubio, and A. R. Solomon, Phys. Rev. **D95**, 043539 (2017), arXiv:1610.01799 [gr-qc].
- [50] V. Vardanyan, Y. Akrami, L. Amendola, and A. Silvestri, (2017), arXiv:1702.08908 [gr-qc].
- [51] R. Trotta, Mon. Not. Roy. Astron. Soc. **378**, 72 (2007), arXiv:astro-ph/0504022 [astro-ph].
- [52] R. Trotta, Contemp. Phys. **49**, 71 (2008), arXiv:0803.4089 [astro-ph].
- [53] Y. Dirian, S. Foffa, N. Khosravi, M. Kunz, and M. Maggiore, JCAP **1406**, 033 (2014), arXiv:1403.6068 [astro-ph.CO].
- [54] A. Barreira, B. Li, W. A. Hellwing, C. M. Baugh, and S. Pascoli, JCAP **9**, 031 (2014), arXiv:1408.1084.
- [55] Y. Dirian, S. Foffa, M. Kunz, M. Maggiore, and V. Pettorino, JCAP **1504**, 044 (2015), arXiv:1411.7692 [astro-ph.CO].
- [56] Y. Dirian, S. Foffa, M. Kunz, M. Maggiore, and V. Pettorino, JCAP **1605**, 068 (2016), arXiv:1602.03558 [astro-ph.CO].
- [57] M. Tegmark, D. J. Eisenstein, and W. Hu, in *Proceedings, 33rd Rencontres de Moriond fundamental parameters in cosmology: Les Arcs, France, Jan 17-24, 1998* (1998) pp. 355–358, arXiv:astro-ph/9804168 [astro-ph].
- [58] D. J. Eisenstein, W. Hu, and M. Tegmark, Astrophys. J. **518**, 2 (1999), arXiv:astro-ph/9807130 [astro-ph].

- [59] P. A. R. Ade *et al.* (Planck), (2015), arXiv:1502.01589 [astro-ph.CO].
- [60] C. Skordis, D. F. Mota, P. G. Ferreira, and C. Boehm, Phys. Rev. Lett. **96**, 011301 (2006).
- [61] A. Barreira, B. Li, C. M. Baugh, and S. Pascoli, PRD **90**, 023528 (2014), arXiv:1404.1365.
- [62] A. Barreira, P. Brax, S. Clesse, B. Li, and P. Valageas, PRD **91**, 063528 (2015), arXiv:1411.5965.
- [63] N. Bellomo, E. Bellini, B. Hu, R. Jimenez, C. Pena-Garay, and L. Verde, JCAP **1702**, 043 (2017), arXiv:1612.02598 [astro-ph.CO].
- [64] M. Baldi, F. Villaescusa-Navarro, M. Viel, E. Puchwein, V. Springel, and L. Moscardini, MNRAS **440**, 75 (2014), arXiv:1311.2588.
- [65] M. Maggiore, (2015), arXiv:1506.06217 [hep-th].
- [66] M. Maggiore, Phys. Rev. **D93**, 063008 (2016), arXiv:1603.01515 [hep-th].
- [67] M. Maggiore, (2016), arXiv:1606.08784 [hep-th].
- [68] M. E. Sousa and R. P. Woodard, Class. Quant. Grav. **20**, 2737 (2003), arXiv:astro-ph/0302030 [astro-ph].
- [69] Y. Dirian and E. Mitsou, JCAP **10**, 065 (2014), arXiv:1408.5058 [gr-qc].
- [70] N. Koshelev, Grav.Cosmol. **15**, 220 (2009), arXiv:0809.4927 [gr-qc].
- [71] T. S. Koivisto, AIP Conf.Proc. **1206**, 79 (2010), arXiv:0910.4097 [gr-qc].
- [72] A. O. Barvinsky, Phys.Rev. **D85**, 104018 (2012), arXiv:1112.4340 [hep-th].
- [73] S. Foffa, M. Maggiore, and E. Mitsou, Phys.Lett. **B733**, 76 (2014), arXiv:1311.3421 [hep-th].
- [74] S. Foffa, M. Maggiore, and E. Mitsou, Int.J.Mod.Phys. A, to appear (2014), arXiv:1311.3435 [hep-th].
- [75] Y. Dirian, S. Foffa, M. Kunz, M. Maggiore, and V. Pettorino, JCAP **4**, 044 (2015), arXiv:1411.7692.
- [76] R. R. Caldwell, M. Kamionkowski, and N. N. Weinberg, Phys. Rev. Lett. **91**, 071301 (2003), arXiv:astro-ph/0302506 [astro-ph].
- [77] A. Codello and R. K. Jain, Int. J. Mod. Phys. **D25**, 1644023 (2016), arXiv:1605.07630 [gr-qc].
- [78] R. R. Caldwell and S. S. Gubser, Phys. Rev. **D87**, 063523 (2013), arXiv:1302.1201 [astro-ph.CO].
- [79] H. Nersisyan, Y. Akrami, L. Amendola, T. S. Koivisto, and J. Rubio, Phys. Rev. **D94**, 043531 (2016), arXiv:1606.04349 [gr-qc].
- [80] N. Aghanim *et al.* (Planck), Astron. Astrophys. **594**, A11 (2016), arXiv:1507.02704 [astro-ph.CO].
- [81] P. A. R. Ade *et al.* (Planck), (2015), 10.1051/0004-6361/201525941, arXiv:1502.01591 [astro-ph.CO].
- [82] F. Beutler, C. Blake, M. Colless, D. H. Jones, L. Staveley-Smith, L. Campbell, Q. Parker, W. Saunders, and F. Watson, MNRAS **416**, 3017 (2011), arXiv:1106.3366.
- [83] A. J. Ross, L. Samushia, C. Howlett, W. J. Percival, A. Burden, and M. Manera, MNRAS **449**, 835 (2015), arXiv:1409.3242.
- [84] L. Anderson and et al, MNRAS **441**, 24 (2014), arXiv:1312.4877.
- [85] M. Betoule and et al, AAP **568**, A22 (2014), arXiv:1401.4064.
- [86] A. Lewis, A. Challinor, and A. Lasenby, Astrophys. J. **538**, 473 (2000), arXiv:astro-ph/9911177 [astro-ph].
- [87] D. Blas, J. Lesgourgues, and T. Tram, JCAP **7**, 034 (2011), arXiv:1104.2933.
- [88] https://github.com/dirian/class_public/tree/nonlocal.
- [89] B. Audren, J. Lesgourgues, K. Benabed, and S. Prunet, JCAP **2**, 001 (2013), arXiv:1210.7183.
- [90] R. H. Becker *et al.* (SDSS), Astron. J. **122**, 2850 (2001), arXiv:astro-ph/0108097 [astro-ph].
- [91] G. Mangano, G. Miele, S. Pastor, T. Pinto, O. Pisanti, and P. D. Serpico, Nucl. Phys. **B729**, 221 (2005), arXiv:hep-ph/0506164 [hep-ph].
- [92] J. Lesgourgues and S. Pastor, Phys. Rept. **429**, 307 (2006), arXiv:astro-ph/0603494 [astro-ph].
- [93] J. Lesgourgues, G. Mangano, G. Miele, and S. Pastor, *Neutrino cosmology* (Cambridge University Press, 2013).
- [94] P. A. R. Ade *et al.* (Planck), Astron. Astrophys. **571**, A16 (2014), arXiv:1303.5076 [astro-ph.CO].
- [95] N. Aghanim *et al.* (Planck), (2016), arXiv:1608.02487 [astro-ph.CO].
- [96] M. Archidiacono, T. Brinckmann, J. Lesgourgues, and V. Poulin, JCAP **1702**, 052 (2017), arXiv:1610.09852 [astro-ph.CO].
- [97] K. P. Burnham and D. R. b. Anderson, *Model selection and multimodel inference : a practical information-theoretic approach* (Springer, New York, 2002) Édition revue et corrigée de : Model selection and inference, cop. 1998.
- [98] G. Efstathiou, Mon. Not. Roy. Astron. Soc. **388**, 1314 (2008), arXiv:0802.3185 [astro-ph].
- [99] S. Alam *et al.* (BOSS), Submitted to: Mon. Not. Roy. Astron. Soc. (2016), arXiv:1607.03155 [astro-ph.CO].
- [100] J. Lesgourgues and S. Pastor, New Journal of Physics **16**, 065002 (2014), arXiv:1404.1740 [hep-ph].
- [101] W. Hu, D. J. Eisenstein, and M. Tegmark, Phys. Rev. Lett. **80**, 5255 (1998), arXiv:astro-ph/9712057 [astro-ph].
- [102] J. Adamek, D. Daverio, R. Durrer, and M. Kunz, JCAP **1607**, 053 (2016), arXiv:1604.06065 [astro-ph.CO].
- [103] D. Inman and U.-L. Pen, Phys. Rev. **D95**, 063535 (2017), arXiv:1609.09469 [astro-ph.CO].
- [104] F. Beutler, C. Blake, M. Colless, D. H. Jones, L. Staveley-Smith, G. B. Poole, L. Campbell, Q. Parker, W. Saunders, and F. Watson, Mon.Not.Roy.Astron.Soc. **423**, 3430 (2012), arXiv:1204.4725 [astro-ph.CO].
- [105] A. Oka, S. Saito, T. Nishimichi, A. Taruya, and K. Yamamoto, Mon.Not.Roy.Astron.Soc. **439**, 2515 (2014), arXiv:1310.2820 [astro-ph.CO].
- [106] C. Howlett, A. Ross, L. Samushia, W. Percival, and M. Manera, (2014), arXiv:1409.3238 [astro-ph.CO].
- [107] C.-H. Chuang, F. Prada, F. Beutler, D. J. Eisenstein, S. Escoffier, *et al.*, (2013), arXiv:1312.4889 [astro-ph.CO].
- [108] L. Samushia, B. A. Reid, M. White, W. J. Percival, A. J. Cuesta, *et al.*, Mon.Not.Roy.Astron.Soc. **439**, 3504 (2014), arXiv:1312.4899 [astro-ph.CO].
- [109] C. Blake, S. Brough, M. Colless, C. Contreras, W. Couch, *et al.*, Mon.Not.Roy.Astron.Soc. **425**, 405 (2012), arXiv:1204.3674 [astro-ph.CO].
- [110] S. de la Torre, L. Guzzo, J. Peacock, E. Branchini, A. Iovino, *et al.*, Astron.Astrophys. **557**, A54 (2013), arXiv:1303.2622 [astro-ph.CO].
- [111] e. a. Amendola, L., Living Reviews in Relativity **16**, 6 (2013), arXiv:1206.1225.
- [112] E. Majerotto, L. Guzzo, L. Samushia, W. J. Percival, Y. Wang, S. de la Torre, B. Garilli, P. Franzetti, E. Rossetti, A. Cimatti, C. Carbone, N. Roche, and G. Zamorani, MNRAS **424**, 1392 (2012), arXiv:1205.6215.
- [113] C. Heymans, L. Van Waerbeke, L. Miller, T. Erben, H. Hildebrandt, H. Hoekstra, T. D. Kitching, Y. Mellier, P. Simon, C. Bonnett, J. Coupon, L. Fu, J. Harnois Déraps, M. J. Hudson, M. Kilbinger, K. Kuijken, B. Rowe, T. Schrabback, E. Semboloni, E. van Uitert, S. Vafaei, and M. Velander, MNRAS **427**, 146 (2012), arXiv:1210.0032.

- [114] K. Kuijken *et al.*, *Mon. Not. Roy. Astron. Soc.* **454**, 3500 (2015), arXiv:1507.00738 [astro-ph.CO].
- [115] S. Joudaki *et al.*, (2016), arXiv:1610.04606 [astro-ph.CO].
- [116] A. Johnson, C. Blake, J. Koda, Y.-Z. Ma, M. Colless, M. Crocce, T. M. Davis, H. Jones, C. Magoulas, J. R. Lucey, J. Mould, M. I. Scrimgeour, and C. M. Springob, *MNRAS* **444**, 3926 (2014), arXiv:1404.3799.
- [117] A. Barreira, A. G. Sánchez, and F. Schmidt, *ArXiv e-prints* (2016), arXiv:1605.03965.
- [118] G. Efstathiou, *MNRAS* **440**, 1138 (2014), arXiv:1311.3461.
- [119] A. G. Riess, L. M. Macri, S. L. Hoffmann, D. Scolnic, S. Casertano, A. V. Filippenko, B. E. Tucker, M. J. Reid, D. O. Jones, J. M. Silverman, R. Chornock, P. Challis, W. Yuan, P. J. Brown, and R. J. Foley, *APJ* **826**, 56 (2016), arXiv:1604.01424.
- [120] A. G. Riess, L. Macri, S. Casertano, H. Lampeitl, H. C. Ferguson, A. V. Filippenko, S. W. Jha, W. Li, and R. Chornock, *APJ* **730**, 119 (2011), arXiv:1103.2976.
- [121] E. M. L. Humphreys, M. J. Reid, J. M. Moran, L. J. Greenhill, and A. L. Argon, *APJ* **775**, 13 (2013), arXiv:1307.6031.
- [122] W. Cardona, M. Kunz, and V. Pettorino, *JCAP* **1703**, 056 (2017), arXiv:1611.06088 [astro-ph.CO].
- [123] V. Bonvin, F. Courbin, S. H. Suyu, P. J. Marshall, C. E. Rusu, D. Sluse, M. Tewes, K. C. Wong, T. Collett, C. D. Fassnacht, T. Treu, M. W. Auger, S. Hilbert, L. V. E. Koopmans, G. Meylan, N. Rumbaugh, A. Sonnenfeld, and C. Spiniello, *ArXiv e-prints* (2016), arXiv:1607.01790.
- [124] V. V. Luković, R. D’Agostino, and N. Vittorio, *ArXiv e-prints* (2016), arXiv:1607.05677.
- [125] J. L. Bernal, L. Verde, and A. G. Riess, *ArXiv e-prints* (2016), arXiv:1607.05617.
- [126] M. C. Gonzalez-Garcia, M. Maltoni, J. Salvado, and T. Schwetz, *Journal of High Energy Physics* **12**, 123 (2012), arXiv:1209.3023 [hep-ph].
- [127] J. D. Vergados, H. Ejiri, and F. Šimkovic, *Reports on Progress in Physics* **75**, 106301 (2012), arXiv:1205.0649 [hep-ph].
- [128] G. Drexlin, V. Hannen, S. Mertens, and C. Weinheimer, *ArXiv e-prints* (2013), arXiv:1307.0101 [physics.ins-det].